Journal of Environmental Management 404 (2026) 129410

Contents lists available at ScienceDirect

Journal of Environmental Management

journal homepage: www.elsevier.com/locate/jenvman

Research article

Dual valorization of sewage sludge ash through phosphorus recovery and wastewater remediation

Praveena Pachaiappan [a], Mattia Massa [a], Laura Riva [b], Arianna De Santis [b], Tatsiana Reishal [c], Andrea D'Anna [c], Marco Blazina [c], Elza Bontempi [a,*], Carlo Punta [b,**]

[a] INSTM and Chemistry for Technology Laboratory, Department of Mechanical and Industrial Engineering, University of Brescia, Via Branze 38, 25123, Brescia, Italy
[b] Department of Chemistry, Materials, and Chemical Engineering "G. Natta" and INSTM Local Unit, Politecnico di Milano, Piazza Leonardo da Vinci 32, I-20133, Milano, Italy
[c] MM SpA, Depuratore Milano San Rocco, Loc. Ronchetto delle Rane, 20141, Milano, Italy

ARTICLE INFO

Keywords:
Sewage sludge ash
Sorption
Organic dyes
Sustainability analysis
Wastewater treatment
Waste valorization

ABSTRACT

Sewage sludge ash (SSA) can be exploited for phosphorus recovery, as it contains about 5–15% of this element by mass. However, residual waste remains and requires valorization to avoid disposal costs. This study investigates fluidized bed mono-combusted ash from sewage treatment for water remediation within a circular economy framework. Acid treatment, primarily applied for phosphorus extraction and recovery, was here followed by the valorization of the residual ash as an adsorbent, since this step simultaneously increases porosity and surface area. Characterization by SEM, BET, XRD, ICP-OES and pH_{PZC} provided insights into structural and chemical changes in SSA and its activated form (ASSA). Results showed complete phosphorus removal, surface area increase from 1.51 to 16.18 m^2/g, and compositional phase modifications. Batch adsorption experiments were performed on solutions mono-contaminated with four anionic organic dyes bearing sulphonate groups and methylene blue as a representative cationic dye. ASSA resulted in being much more effective in the removal of the anionic dyes, with the adsorption efficiency gap increasing at higher contaminants' concentrations, while no significant difference was observed in the adsorption of methylene blue. Isotherms and kinetics of the decontamination processes allowed elucidating the adsorption mechanisms, which differ for different dyes and in some cases between SSA and ASSA. Sustainability analysis, using the ESCAPE tool, indicates that the produced adsorber may be competitive with activated carbons in terms of overall environmental impact, despite its lower adsorption efficiency. The successful regeneration and reuse of ASSA is contingent upon the types and levels of contaminants present.

1. Introduction

In wastewater treatment plants, sewage undergoes comprehensive purification processes to remove contaminants. The residual solids from this treatment, known as sludge, can be incinerated, transforming into ash, a practice that necessitates careful management due to potential environmental and health considerations. Sewage sludge ash (SSA) is increasingly recognized as a secondary phosphorus (P) resource for fertilizer production, with reported P contents of 4–13% (dry mass), comparable to low-grade phosphate rock (Boniardi et al., 2022). Global SSA generation is estimated at approximately 1.7 million t per year, yet a large fraction is still landfilled rather than valorized (Chen et al., 2024). For instance, the recovery potential of P from SSA in Germany alone has been estimated at about 19,000 t per year (Herzel et al., 2016). For this reason, SSA could represent an important alternative to the primary P source (phosphate rocks), which is becoming more and more a critical raw material, also due to recent geopolitical events (Zanoletti et al., 2021). Nevertheless, the bioavailability of phosphorus in SSA is often poor, and more than half of the ash cannot be used as fertilizer due to its high heavy metal content (Herzel et al., 2016). For this reason, studies on P recovery from SSA have primarily concentrated on enhancing the efficiency of P extraction and its purification while managing undesirable metals. Chemical washing stands out as the most widely used technique for this purpose, due to the simplicity and cost-effectiveness of

* Corresponding author.(E.B.).
** Authors to whom correspondence should be addressed: (C.P.)
E-mail addresses: elza.bontempi@unibs.it (E. Bontempi), carlo.punta@polimi.it (C. Punta).

https://doi.org/10.1016/j.jenvman.2026.129410
Received 8 January 2026; Received in revised form 13 February 2026; Accepted 16 March 2026
Available online 28 March 2026

the process (Biswas et al., 2009). Typically, inorganic acids, such as H_2SO_4, have demonstrated higher efficiency in P extraction (Boniardi et al., 2021). According to this approach, after P leaching under acidic conditions, a chemical precipitation is generally promoted to recover this element in the phosphate form from the liquid phase. Ca^{2+} or Mg^{2+} are the prevailing precipitators, leading to the formation of hydroxyapatite or struvite, correspondingly (Ye et al., 2017). However, heavy metals may also co-precipitate with P and risk contaminating the precipitate (Muryanto and Bayuseno, 2014). For this reason, leachate pre-treatments can be necessary to remove metals before promoting precipitation (Boniardi et al., 2024). Besides the recovery of P, some characteristics of SSA make this waste interesting for other potential applications. For example, the amorphous content in SSA (Lynn et al., 2015), which is reported to be higher than 35%, implies that this by-product can exhibit some reactivity so that it can serve as a component in cement or as a stabilizer for heavy metals (Benassi et al., 2019).

Another potential application would consist of the use of SSA as a sorbent for water treatment. Adsorption occurs through physical or chemical processes, where surface energy and irregular attractive forces on the adsorbent draw in the adsorbate, balancing stable and excess forces (Abbas et al., 2018; Hessou et al., 2019). Materials derived from waste sources hold significant importance due to their abundant availability and often low cost and for this reason, they are widely investigated as potential sorbents of contaminants. Nevertheless, their utilization typically necessitates various treatments to achieve the essential characteristics of the final product, such as increasing the surface area, and/or mitigating potential contamination risks associated with their origin. This may compromise the sustainability of the obtained final material, as extensively discussed in a recent work, which presents a tool for preliminary sustainability evaluation of new materials (Ducoli et al., 2023).

Some research studies have already explored the adsorption capacity of fly ash (FA) by surface modification. In 2020, Chen et al. reported the FA treatment by HCl and NaOH, observing for the treated products a rougher surface with more adsorption sites for target norfloxacin (Chen et al., 2020). In another study, FA was pre-treated with nitric acid before undergoing surface modification by vinyltriethoxysilane (VTES) grafting, which brought about significant alterations to ash surface properties (Trong et al., 2015). Surface modification can enhance the adsorption capacity of FA by several mechanisms. In particular, it has been shown that acid treatment can lead to an increase of the specific surface area, providing more active sites for adsorption. Moreover, it can also alter the surface charge, favouring the adsorption of positively charged pollutants (Singh et al., 2020).

Nevertheless, similar studies are very limited for SSA, being mainly focused on the adsorption of heavy metals, in particular Cu(II), Cd(II), and Zn(II) (Gao et al., 2021; Wang et al., 2019). Although the surface charge and cation-exchange capacity of SSA were found to be lower than those of some natural minerals (Pan and Tseng, 2001), SSA should be considered as a potential organic-pollutant adsorbent. Moreover, working on municipal SSA highly limits the risk of possible contaminants' release in the water medium due to the incineration process, which reduces the organic pollutants and pathogens. Despite these promising advantages, to the best authors' knowledge, the possible use of SSA as a dye adsorber has never been investigated in the literature.

The global industry produces over 7×10^7 tons of dyes annually because the textile sector consumes an estimated minimum of 10,000 tonnes of them each year (Al-Tohamy et al., 2022). The extensive water usage in fabric production leads to significant volumes of wastewater characterized by elevated concentrations of dissolved solids, organics, metals, salts, and persistent synthetic dyes (Ismail and Sakai, 2022). Due to their robust durability and solubility in water, conventional treatment methods often prove inadequate in effectively addressing this issue (Shindhal et al., 2021). As secondary pollution and incomplete removal of organic contaminants persist following discoloration, there arises a need for the adoption of advanced methodologies to address these challenges effectively (Samsami et al., 2020). Moreover, synthetic dyes are prevalent in diverse industries like food, rubber, cosmetics, and textiles, often ending up in wastewater during production. Their removal before environmental discharge is crucial due to potential toxicity to aquatic ecosystems (Riva et al., 2020).

In this work, we propose for the first time the use of SSA as an adsorbent for different organic dyes. The approach exploits the acidic treatment carried out for phosphorus extraction and recovery, after which the remaining solid (ASSA) is valorized as an activated adsorbent, with enhanced surface area and porosity. In this way, phosphorus is first recovered as a critical raw material, and the subsequent use of the residual solid enables a closed-loop valorization pathway.

The investigation was conducted on SSA, both before and following activation procedures, facilitated by an innovative incineration research facility operating within a wastewater treatment plant located in Milan, Italy. We investigated the sorption efficiency towards five commonly utilized organic dyes (Fig. S1), both anionic and cationic ones, namely Naphthol Blue Black (NBB), Orange II Sodium Salt (OSS), Brilliant Blue R (BB), Cibacron Brilliant Yellow (CBY), and Methylene Blue (MB). Despite sharing a similar structural framework, these dyes exhibit variations in molecular weight and the number of sulphate functional groups. After an in-deep characterization of materials, their adsorption efficiency has been investigated by isothermal and kinetic studies.

2. Materials and methods

2.1. General

All the reagents and dyes were purchased from Sigma-Aldrich, Carlo Erba and Fluorochem. Deionized water was produced with a Millipore Elix® Deionizer with Progard® S2 ion exchange resins. UV spectra and data were recorded on a V-600 Series UV-vis spectrophotometer from JASCO (Cremella (LC), Italy). Other equipment used in the procedure is Heidolph multi-reax shaker (Schwabach, Germany) equipped with a 12-rack carousel. Scanning electron microscopy (SEM) was performed using a variable-pressure instrument (SEM Cambridge Stereoscan 360) at 100/120 pA with a detector BSD. Quantitative analysis of the samples was performed using Inductively Coupled Plasma Optical Emission Spectroscopy (ICP-OES) with a PerkinElmer Optima model 8300 instrument.

2.2. SSA production

SSA samples were produced and provided by MM S.p.A, at the wastewater treatment plant of Milano San Rocco, Italy. In this site, a mono-combustion sludge fluidized bed was installed by FMI Process, France. The plant installed in San Rocco has different potentials depending on the feed material. In the present work, it operated by processing dehydrated sludge (20-24% dry matter) up to 19 t/day in feed, under the operating conditions of 700-750 °C and post-combustion at 850 °C and a residence time of 2-3 s.

After passing through two heat exchangers (air-air and air-water) the fumes were treated by two sets of bag filters; the resulting SSA after combustion was collected by low-density polyethylene bags of 850-900 kg capacity. Ash production was approximately 8-12% of the feed material.

2.3. P recovery by SSA activation

SSA was subjected to two rounds of washing with deionized water and subsequently oven-dried at 110 °C overnight before being sieved through a 150 μm mesh (sieve no. 100). For P extraction and SSA activation, 40 g of sample were refluxed in 250 mL of 40 wt% H_2SO_4 at 67 °C for 4 h in a round-bottom flask. The resulting slurry was air-cooled and filtered through a sintered glass fibres filter. The filter cake underwent three washes with 250 mL of hot (60 °C) deionized water until the filtrate reached neutrality (Ahmad et al., 2007). The acid-treated ash is

hereinafter named acid SSA (ASSA). Scheme 1 depicts the activation procedure for SSA.

Acid treatment of SSA produces residual ASSA and a filtrate. The acid filtrate was analysed by ICP-OES to quantify the leached phosphorus content.

2.4. Adsorbents characterization

For the evaluation of the P content, the SSA was digested by using a mixture of concentrated acids 2:1/H_2SO_4:HNO_3, following the procedure reported in Fiameni et al. (2021), using the absorbance signal of the resulting solution at a wavelength of 700 nm to quantify the P content. The analysis was performed with a spectrophotometer Hach Lange DR 3800.

The pH drift method was used to measure the point of zero charge (pH_{PZC}) of SSA and ASSA, which is the pH above which the entire surface of the sorbent materials is negatively charged (Lopez-Ramon et al., 1999). To achieve these data, a Falcon vial containing 10 mL of a 0.01 M NaCl solution was utilized, and nitrogen (N_2) was blown into the solution to stabilize the pH by preventing the absorption of CO_2. Subsequently, the pH was adjusted to predetermined initial values ranging from 2 to 12 by adding either 0.01 N HCl or 0.01 N NaOH. Following this approach, 0.03 g of the sorbent were introduced into the solution. After 48 h, the final pH was determined and plotted against the initial pH. The pH at which the curve intersected the bisector $pH_{(final)} = pH_{(initial)}$ delineated the pH_{PZC} of the specific sorbent.

The specific surface area of the adsorbents was determined using the Brunauer-Emmett-Teller (BET) (Micromeritics® TriStar II Plus) analysis. SEM was used to characterize the morphology of SSA and ASSA. X-Ray Diffraction (XRD) measurements were realised by a PANalytical X'Pert PRO diffractometer (PANalytical, Malvern, UK), equipped with a Cu Kα anode and operating at a voltage of 40 kV and a current of 40 mA. For the phase identification, Philips X'Pert software, associated with the Crystallography Open Database (COD), was used, as described in literature (Assi et al., 2019). Rietveld analysis, with an internal standard, was used to quantify the crystalline phases and the amorphous content in the SSA (De La Torre et al., 2001). The XRD measurements were conducted for both SSA and ASSA.

2.5. Sorption tests

Sorption tests were conducted by contacting 12 mg of SSA or ASSA with 15 mL of aqueous solutions containing the different dyes for 24 h in a Falcon vial, both under static conditions and in an orbital shaker at room temperature (Riva et al., 2020). The concentrations of dyes for preliminary adsorption tests chosen were 5 mg/L, 50 mg/L, 150 mg/L. Each experiment was reproduced in triplicate. After 24 h of sorption, each sample was analysed by UV-vis spectrophotometer technique.

UV-vis spectra, characteristic λ_{max}, and calibration lines for all five dyes are reported in the Supplementary Material (SM, Figs. S3–S12).

2.5.1. Isotherms and kinetics

Isotherm and kinetic sorption tests were conducted at room temperature (25 °C) in dynamic conditions, with the orbital shaker operating at 450 rpm.

Isotherm experiments were performed by maintaining a constant dose (sorbent quantity/solution volume ratio) of 0.8 mg/mL for 24 h while varying the dye concentration in each solution. For each dye, nine distinct concentrations were tested, with three trials conducted for each concentration. The absorbance of the solutions was measured by a UV-vis spectrophotometer at both time zero and after 24 h.

Kinetic tests were conducted under dynamic conditions at room temperature, following the protocol previously described for isotherm tests, fixing the initial concentration for each dye at 20 mg/L. Solutions underwent orbital shaking and were sampled and analysed after 1, 2, 3, 4, 5, 6, 8, and 24 h.

2.6. Regeneration and reusability studies

Experiments were undertaken to assess the potential reuse of the ASSA. Initially, the adsorbed ash was retrieved post-adsorption by allowing the ash to interact with a solution containing the selected dye (20 mg/L dye concentration, 15 mL of dye solution, 12 mg of ASSA). Subsequently, the mixture was filtered using a Büchner funnel and rinsed with deionized water.

Preliminary regeneration tests considered both 0.1 M HCl_{aq} and 0.1 M $NaOH_{aq}$ as potential desorption solutions. 20 mg of post-adsorption ASSA were immersed in 20 mL of the selected solutions, under dynamic conditions (450 rpm) at room temperature (25 °C) for 24 h.

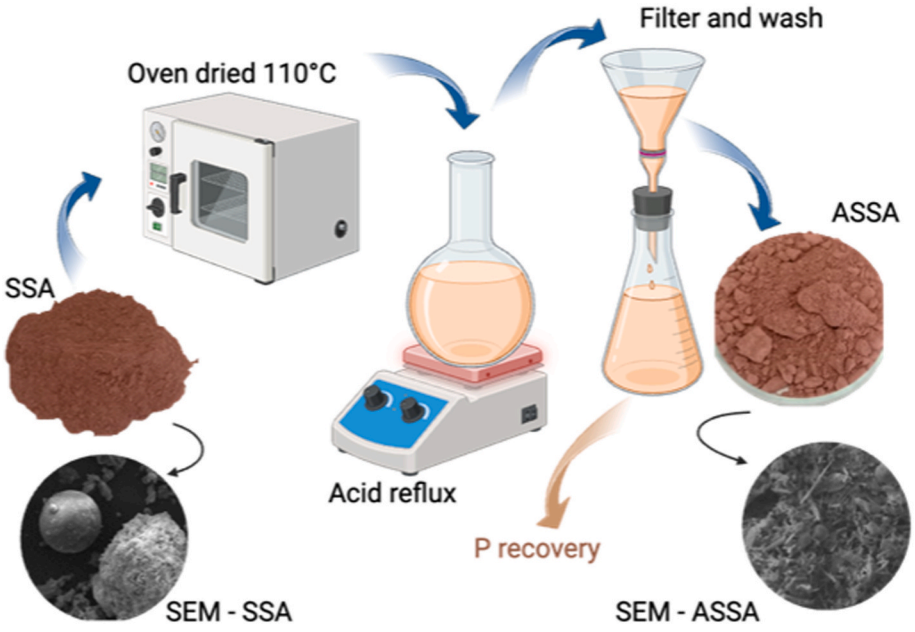

Scheme 1. Activation protocol for SSA.

Following the initial results, which confirmed the regeneration efficiency only using the HCl solution, three distinct molar concentrations of HCl (0.5 M, 0.1 M, and 0.05 M) were compared using the same desorption procedure.

For reusability, tests were conducted on OSS as a representative dye. Regenerated ASSA underwent a sorption step according to the procedure previously described (Section 2.5.1). After the sorption phase, ASSA was vacuum filtered, air-dried, and subjected to a new regeneration cycle, conducted with a 0.1 M HCl solution. Five cycles of sorption-desorption were conducted in triplicate.

3. Results and discussion

3.1. Ash treatment for P extraction and activation

The activation process for SSA followed the protocol depicted in Scheme 1.

SEM analyses allowed a morphological comparison between SSA (Fig. 1A) and its activated form ASSA (Fig. 1B). SSA consisted of particles with different sizes, ranging from a few to more than 100 μm. Most of the particles were spherical, with some of them having additional agglomerated small particles dispersed on their surface. After acidic treatment, ASSA exhibited a remarkably higher micro-porosity and a distinct fibrous structure, with an agglomeration of irregular particles with different shapes and sizes, significantly smaller than those observed in SSA, and rough because of the corrosivity of the treatment. This evidence showed that the modification of SSA by acid treatment led to the opening of pores, increasing the specific surface area of ASSA. These considerations are in accordance with the results obtained by BET (Brunauer-Emmett-Teller) analysis, with surface values moving from 1.51 m^2/g for SSA to an order of magnitude higher equal to 16.18 m^2/g for ASSA.

This enhancement in surface area is indicative of the effectiveness of the acid activation process in generating a highly porous structure in the material, underscoring its potential for various applications, such as adsorption and catalysis (Lee et al., 1982; Yin et al., 2020). Moreover, these results agree with literature data, even if obtained for different ash substrates (Aslam et al., 2019; Losey et al., 2018).

XRD analysis of SSA is reported in Table 1 and Fig. S2A in Supplementary Material. The main crystalline phases were whitlockite, quartz, hematite, calcite, and anhydrite, which are common crystalline phases also detected in SSA obtained from other different sources (Donatello et al., 2010). The high hematite content can be attributed to the use of ferric chloride in the largest sewage treatment facility for the chemically assisted primary sedimentation process.

Table 1 also shows how the amorphous contribution represents more than the 40 $\%_{w/w}$, in agreement with the few available literature data, which report an amorphous phase ranging from 35 to 75$\%_{w/w}$ for this waste (Lynn et al., 2015).

Table 1
SSA and ASSA phase quantification based on Rietveld analysis.

Phase	Chemical formula	Amount ($\%_{w/w}$) SSA	Amount ($\%_{w/w}$) ASSA
Quartz	SiO_2	11.00	15.6
Calcite	$CaCO_3$	7.90	-
Anhydrite	$CaSO_4$	7.40	52.7
Hematite	Fe_2O_3	10.20	1.7
Whitlockite	$Ca_9(MgFe)(PO_4)_6PO_3OH$	10.30	-
Berlinite	$AlPO_4$	0.90	-
Hydroxyapatite	$Ca_5(PO_4)_3OH$	2.60	-
Peroxodiphosphate	$K_4(P_2O_8)$	1.90	-
Tridymite	SiO_2	1.70	-
Anorthite	$CaAl_2Si_2O_8$	2.80	-
Portlandite	$Ca(OH)_2$	0.67	-
Lime	CaO	0.76	-
Goethite	FeO(OH)	1.10	-
Albite	$NaAlSi_3O_8$	-	5.1
Gypsum	$CaSO_4{\cdot}2H_2O$	-	4.9
Talc	$Mg_3Si_4O_{10}(OH)_2$	-	1
Amorphous		40.80	19

The amorphous contribution is generally attributed based on a qualitative point of view, using the apparent intensity of the halo in the XRD patterns (Mahieux et al., 2010). Moreover, a weak intensity of the background may involve an important amount of an amorphous phase. This can be due to the composition of the amorphous phase: the halo intensity is affected by the presence/absence of X-ray absorbing elements. For example, considering a constant quantity, amorphous phases containing Al and/or Si will involve higher scattering intensity in comparison to those containing higher amounts of K and/or Ca (Li et al., 2006; Sulistiyo et al., 2017; Wang et al., 2006).

XRD results of ASSA after the above-described activation procedure are also reported in Table 1 and Fig. S2B. The analysis revealed the formation of higher concentrations of gypsum ($CaSO_4{\cdot}2H_2O$, Equation (1)), renowned for its high surface area and porosity, and anhydrite ($CaSO_4$) (Gitari et al., 2008), with similar characteristics. The intricate composition and lattice structure of gypsum and anhydrite furnish ample active sites for adsorption, facilitating the entrapment of various contaminants present in water media (Hassan et al., 2021; Raii et al., 2014).

$$CaCO_3 + H_2SO_4 \rightarrow CaSO_4 + CO_2 + H_2O \quad (1)$$

Moreover, XRD analysis of ASSA confirmed the effective removal of phosphorus during acid treatment. Mass balance calculations showed that most of the phosphorus initially present in SSA was transferred to the leachate, enabling its recovery in line with established precipitation processes, while the resulting phosphorus-depleted solid (ASSA) was subsequently exploited as an adsorbent. In particular, the SSA contained 8.1 $\%_{w/w}$ P, which after acid treatment decreased to 0.12 $\%_{w/w}$ (value

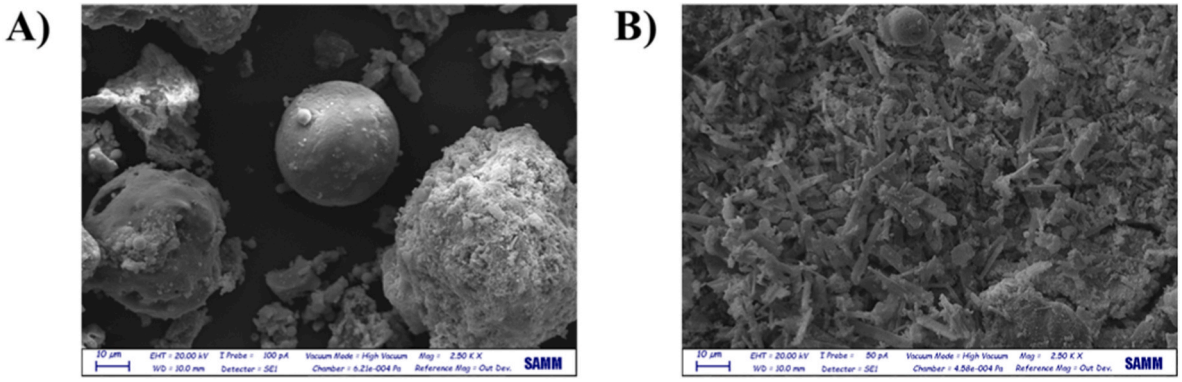

Fig. 1. A) SEM image of SSA, B) SEM image of ASSA.

detected for ASSA).

Finally, the pH_{PZC} was determined for both SSA and ASSA, resulting in values of 11.39 and 9.11, respectively (Fig. S13 in SM). Interestingly, while the value decreased in ASSA as expected, it still maintained significantly over 7, despite the acidic pre-treatment. These results indicated an alkaline nature for the materials, signifying a prevailing positive surface charge at neutral pH.

3.2. Sorption tests

The ashes adsorption performances were first evaluated in preliminary sorption tests carried out at initial dyes' concentrations of 5 mg/L, 50 mg/L and 150 mg/L. Results are reported in Table S1 and Fig. 2. Deionized water solutions containing the selected organic dyes were put in contact with SSA and ASSA to determine the optimal conditions for contaminant removal.

Except for OSS at lower concentrations (5 mg/L), in all the other cases ASSA adsorption efficiency resulted in being clearly higher than that of SSA (Fig. 2). These preliminary results appear to be extremely promising in suggesting that the acid treatment carried out on the SSA has increased their adsorption capacity towards the dyes tested.

For further investigation and comparison of the efficiency of SSA and ASSA as sorbent systems, isotherm experiments were conducted. Final data sets were analysed considering non-linearized methods, in particular the Langmuir model (Equation (2)) and the Freundlich model (Equation (3)) (Foo and Hameed, 2010).

The Langmuir model describes sorption on a homogeneous surface with a finite number of identical sites, ideal for monolayer-localized adsorption. The Freundlich model is an empirical isotherm that accounts for adsorption on heterogeneous surfaces, allowing for multilayer formation and variable adsorption energies across sites (Bonilla-Petriciolet et al., 2017). All collected data, along with the isotherm fittings for OSS, NBB, CBY, BB, and MB, are comprehensively depicted in Fig. 3, for both SSA (Fig. 3A) and ASSA (Fig. 3B). Tables S2 and S3 report the best model fittings for each dye.

$$qe = \frac{Q_{max} K C_e}{1 + K C_e} \tag{2}$$

$$qe = K_F * C_e^{\frac{1}{n}} \tag{3}$$

The adsorption data for OSS and NBB were best fitted by the Langmuir isotherm model, indicating a monolayer adsorption on a homogeneous surface. In both cases ASSA, showed a Qmax almost double for OSS and three times higher for NBB with respect to SSA (Tables S2 and S3).

This increase in adsorption capacity can likely be attributed to the larger exposed surface area observed for ASSA compared to SSA.

In contrast, the BB dataset demonstrated better fitting with the Freundlich model for SSA and ASSA data, suggesting a different sorption mechanism given by a different interaction between the sorbent's surface and the BB molecules. In this case, there was a modest improvement in sorbent performance from SSA ($Q_{max} = 13$ mg/g) to ASSA ($Q_{max} = 17$ mg/g), with a less pronounced gap than that observed for OSS and NBB. This is probably due to the different solute-adsorbent interaction, which also influences the sorption performance of the materials.

Results obtained with the CBY dye in the presence of SSA deserve attention. No acceptable fitting could be obtained for the adsorption data, neither by applying the Langmuir equation nor the Freundlich one. This phenomenon could be ascribed to the fact that solute-solute interactions clearly prevail over the solute-sorbent ones, making it impossible to calculate a correct Qmax. A similar phenomenon for CBY was already observed with other sorbent systems (Riva et al., 2020). As shown in Fig. 3 (A), CBY and OSS exhibit broadly similar removal efficiency; however, since isotherm models could not be fitted to CBY, the maximum adsorption capacity (Qmax) could not be determined.

A different situation is observed for the data collected with ASSA, where it was possible to obtain a good fit ($R^2 = 0.99$) with Langmuir's model, resulting in a Q_{max} of 15 mg/g. In this case, the chemical modification of ASSA composition probably favoured the solute-sorbent interaction.

Concerning the only cationic dye under study, methylene blue (MB), what could be observed was that both data with SSA and data with ASSA were analysed obtaining good fits, but in this case with different adsorption mechanisms moving from SSA to ASSA. In fact, the best fitting for the SSA data was Freundlich's, with an uptake of around 6 mg/g. With the ASSA data, the best fitting was obtained with the Langmuir equation, without obtaining an increase in terms of Q_{max}, which remained around 6 mg/g.

The organic dyes under investigation differ for two crucial parameters, which are the number of sulfonate units in their molecular structure and their molecular size. While we would expect that the more the sulphonate units, the higher should be the electrostatic interaction with the adsorbent, we should consider that the molecules' shapes and dimensions could also play a significant role in determining solute diffusivity within the adsorbent material.

In fact, in the presence of ASSA, dyes with lower molecular weights exhibited progressively higher adsorptive interactions than those with higher molecular weights, as observed by moving from the relatively small OSS to NBB and further to BB and CBY, the latter two with close molecular weights and similar adsorptive behaviours. On the other side, MB, which is characterized by a positive charge, was poorly adsorbed, due to the lower affinity with the positively charged surface of both SSA and ASSA, as resulted by pH_{PZC} previously discussed. In general, with SSA, adsorption behaviour and capacity were irregular and lower overall for all dyes.

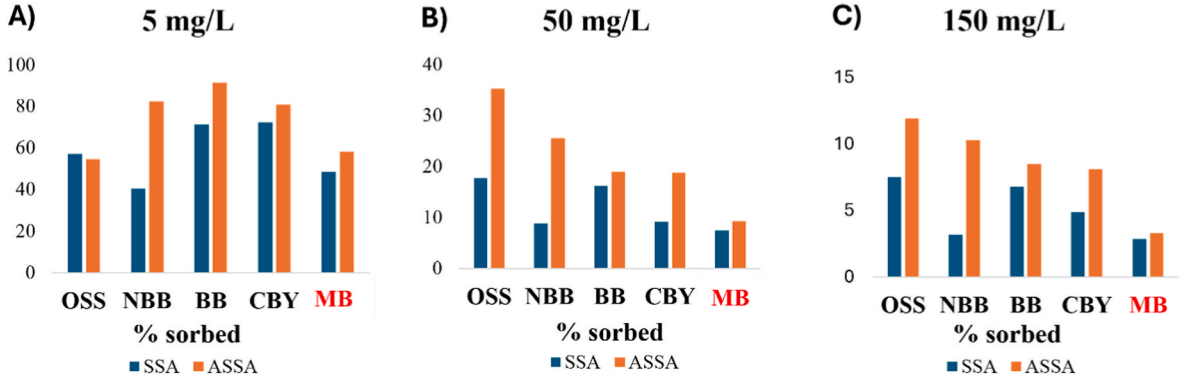

Fig. 2. Preliminary sorption tests with dyes at initial concentrations of A) 5 mg/L, B) 50 mg/L, C) 150 mg/L.

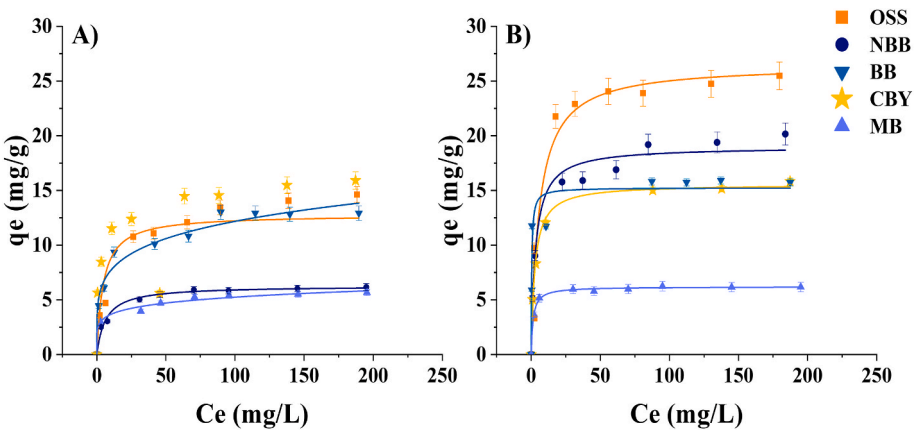

Fig. 3. A) Isotherm fittings of dyes in SSA, B) Isotherm fittings of dyes in ASSA.

3.3. Kinetics

All kinetic studies were conducted on both SSA and ASSA by fixing dye concentration at 20 mg/L and maintaining a constant dose, using the same ratio used in isotherm studies. Results are reported in Fig. 4 and Tables S4–S5 in SM. The datasets of all dyes and two ashes fit with pseudo-second order kinetics, represented by Equation (4), which implies that the adsorption process is more dependent on the availability of adsorption sites than the concentration of the adsorbate itself, indicating a chemisorption effect. Although both SSA and ASSA follow a pseudo-second-order kinetic model, ASSA reaches the adsorption plateau more rapidly than SSA. Specifically, SSA attains 90% of Qe after 6 h, whereas ASSA requires only 4 h, confirming the faster kinetics of ASSA compared to SSA.

$$\frac{dq_t}{dt} = k_2\left(q_{eq} - q_t\right)^2 \quad (4)$$

3.4. Desorption and reusability tests

As previously discussed, the activation of ash underlined the necessity of acidic treatment to effectively open the sorbent's pore structure, increasing the surface area and modifying the chemical composition of ash, thereby facilitating pollutant adsorption.

Considering the importance of regenerating and reusing adsorbent materials, regeneration tests in alkaline and acidic environments, followed by reusability assessment testing of multiple sorption-desorption cycles, were conducted to evaluate this aspect.

Acidic treatment (0.1 M HCl) proved to be the most suitable approach for ASSA regeneration, enabling its potential reuse. In contrast, alkaline treatment did not provide any regeneration capability, which was consistent with the higher adsorption capacity of ASSA observed under basic conditions. According to the results obtained, 0.1 M HCl was employed as the regenerating agent for all dye-loaded ASSA samples.

The reusability assessment was conducted considering five adsorption-desorption cycles to gauge the impact of repeated regeneration on the sorption efficiency of ASSA. The results are presented in Table S6 in SM.

The regeneration procedure proved to be effective in the adsorption tests with OSS and BB, where ASSA retained approximately 85% of their original adsorption capacity after five reusability cycles. In contrast, with CBY and NBB ASSA exhibited the lowest reusability efficiency, with only about 50% of its initial adsorption capacity preserved. Lastly, MB displayed an irregular behaviour in the reusability test, reaching final adsorption values of around 60% of the initial value.

Overall, the regeneration–reuse experiments revealed that, even under the least favorable conditions, ASSA maintained adsorption capacities above 50% after five consecutive cycles. These findings demonstrate that ASSA could be effectively reused after a regeneration process carried out under acidic conditions.

3.5. Sustainability analysis

The ESCAPE method, formally known as the Evaluation of Sustainability of material substitution using CArbon footPrint by a simplifiEd approach (Ducoli et al., 2023), provides a valuable tool for material scientists to assess and compare the sustainability of material synthesis at the lab scale. This method focuses specifically on evaluating the

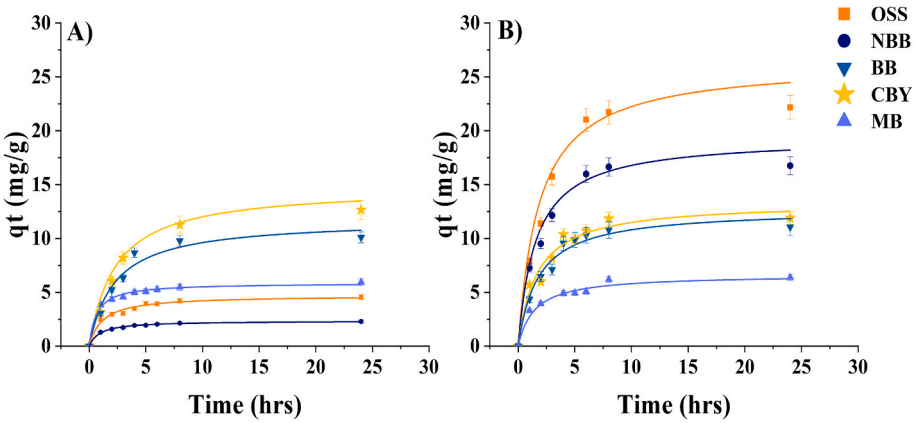

Fig. 4. A) Kinetic behaviour of SSA, B) Kinetic behaviour of ASSA.

sustainability of new materials by comparing their synthesis processes to those of natural resources or corresponding commercial chemicals. The primary aim is to quantify sustainability through embodied energy (EE) and CO_2 footprint (CF), two typical Life Cycle Assessment (LCA) indicators, thus offering a less resource-intensive tool when full LCA data are unavailable (Bontempi, 2023). By evaluating all steps in the synthesis process, including chemical, mechanical, and thermal treatments, ESCAPE allows for customization and focuses on significant energy and emission contributions. This approach supports eco-design by identifying the most energy-intensive steps in the synthesis (Nicastro et al., 2025). It serves as a preliminary screening tool to evaluate material sustainability before conducting a full LCA, aiding early decision-making in the development of eco-friendly technologies (Bontempi, 2017).

ESCAPE approach acts as a valuable preliminary screening tool to determine the viability of new materials, facilitating early, informed decision-making in the development of eco-friendly technologies (Ducoli et al., 2023).

In this study, this method was used to evaluate the sustainability of the proposed procedure by comparing the energies and emissions involved in the synthesis with the corresponding values needed to obtain activated carbon (AC). EE and CF, necessary to produce 1 kg of activated sewage sludge ash (ASSA), starting from sewage sludge ash (SSA), were calculated. Table 2, with data on chemicals and water usage provided in the supporting materials (Table S7 in SM), reports the results of EE and CF evaluation. To produce 1 kg of AC, average energy demand and average greenhouse gas emissions were calculated as 97 MJ/kg and 6.6 kg CO_2eq/kg (Alhashimi and Aktas, 2017). Then, the ESCAPE index for the proposed ASSA resulted in 0.38. A positive ESCAPE index indicates that the newly proposed material is more sustainable than the chosen reference material, which in this case is AC, making the proposed strategy very interesting. Moreover, literature shows that activated carbon displays higher adsorption efficiency (Riva et al., 2020) compared to ASSA, so it may still be regarded as the more sustainable option in terms of adsorption efficiency normalized to EE of CF. Nevertheless, it should be emphasized that the production of ASSA has so far only been evaluated at the laboratory scale and thus offers significant room for optimization; for instance, by avoiding the overnight thermal treatment, it would be possible to lower energy consumption to activate SSA by about 40%. Moreover, the valorization of SSA — a waste otherwise destined for disposal—represents a key advantage of the proposed approach, as it enables phosphorus recovery while simultaneously providing a secondary adsorbent. This dual outcome aligns with circular economy principles and supports the sustainable management of critical resources.

4. Conclusions

This study highlighted the potential of fluidized bed monocombusted ash from sewage water treatment as a viable option for water remediation within a circular economy framework. Acid treatment, primarily applied for phosphorus recovery, was followed by the valorization of the phosphorus-depleted residual ash (ASSA) as an adsorbent. This dual strategy not only ensures the recovery of a critical raw material but also enhances the surface area and adsorption capacity of the remaining solid, enabling the removal of five representative organic dyes commonly used in the textile industry. The adsorption was particularly effective in basic pH, suggesting potential intermolecular interactions and electrostatic interactions between ashes' surface and sulfonated groups of the dyes. Characterization studies further elucidated the structural and surface modifications responsible for these improvements, while regeneration tests confirmed the possibility of reusing the material under acidic conditions.

From a sustainability perspective, the ESCAPE analysis revealed that ASSA may be competitive with commercial activated carbon, despite its lower intrinsic adsorption capacity. Although the ASSA material exhibits an improved adsorption capacity compared to SSA, its overall performance for dye removal remains lower than that of commercial activated carbon. However, preliminary results suggest how ASSA could offer the advantage of potential applicability for metal adsorption, which is not feasible with conventional activated carbon. Future work could therefore focus on exploring ASSA's effectiveness for a wider range of contaminants. Moreover, ASSA powder stabilization in purposely designed formulations would allow its safer use for environmental applications. These results underline the relevance of waste-derived sorbents in sustainable water management and resource recovery, paving the way for future developments that integrate pollution control with circular economy strategies.

Table 2
EE and CF evaluation for all the steps to produce 1 kg of ASSA. To produce 1 kg of AC, average energy demand (EE) and average greenhouse gas emissions (CF) were calculated as 97 MJ/kg and 6.6 kg CO_2eq/kg (Alhashimi and Aktas, 2017; Ducoli et al., 2022).

Process	Embodied energy (MJ/kg)	Carbon footprint ($kgCO_{2\text{-}eq}$/kg)
Chemicals	22.9	0.5
Thermal treatment	32.6	1.4
Water usage	0.1	0.0
TOTAL	55.7	2.0

CRediT authorship contribution statement

Praveena Pachaiappan: Writing – original draft, Validation, Methodology, Investigation, Formal analysis, Data curation, Conceptualization. **Mattia Massa:** Methodology, Formal analysis, Data curation. **Laura Riva:** Writing – review & editing, Visualization, Validation, Investigation, Data curation. **Arianna De Santis:** Validation, Methodology, Formal analysis, Data curation. **Tatsiana Reishal:** Methodology, Formal analysis, Data curation. **Andrea D'Anna:** Supervision, Resources, Project administration, Conceptualization. **Marco Blazina:** Resources, Project administration, Conceptualization. **Elza Bontempi:** Writing – review & editing, Supervision, Resources, Investigation, Funding acquisition, Conceptualization. **Carlo Punta:** Writing – review & editing, Visualization, Supervision, Project administration, Funding acquisition, Conceptualization.

Declaration of competing interest

The authors declare that they have no known competing financial interests or personal relationships that could have appeared to influence the work reported in this paper.

Acknowledgements

This study received funding from the European Union Next-GenerationEU (National Recovery and Resilience Plan_NRRP): Mission 4, Component 2, Investment 1.3_D.D. 1243 2/8/2022, PE0000005 (RETURN Extended Partnership). This work was also supported by RHIGUS (Low Energy Technologies for Recovery of High-Grade Phosphorus) financed by MUR: PRIN 2022. E.B., C.P. and P.P. thank MM SpA and the NRRP project (Mission 4, Component 2, Investment 3.3_D.M. 352 09/04/2022) for co-financing the PhD fellowship of P.P.

Appendix A. Supplementary data

Supplementary data to this article can be found online at https://doi.org/10.1016/j.jenvman.2026.129410.

Data availability

Data will be made available on request.

References

Abbas, K., Znad, H., Awual, M.R., 2018. A ligand anchored conjugate adsorbent for effective mercury(II) detection and removal from aqueous media. Chem. Eng. J. 334. https://doi.org/10.1016/j.cej.2017.10.054.

Ahmad, A.A., Hameed, B.H., Aziz, N., 2007. Adsorption of direct dye on palm ash: kinetic and equilibrium modeling. J. Hazard. Mater. 141, 70–76. https://doi.org/10.1016/J.JHAZMAT.2006.06.094.

Alhashimi, H.A., Aktas, C.B., 2017. Life cycle environmental and economic performance of biochar compared with activated carbon: a meta-analysis. Resour. Conserv. Recycl. 118, 13–26. https://doi.org/10.1016/J.RESCONREC.2016.11.016.

Al-Tohamy, R., Ali, S.S., Li, F., Okasha, K.M., Mahmoud, Y.A.G., Elsamahy, T., Jiao, H., Fu, Y., Sun, J., 2022. A critical review on the treatment of dye-containing wastewater: ecotoxicological and health concerns of textile dyes and possible remediation approaches for environmental safety. Ecotoxicol. Environ. Saf. 231, 113160. https://doi.org/10.1016/J.ECOENV.2021.113160.

Aslam, Z., Hussein, I.A., Shawabkeh, R.A., Parvez, M.A., Ahmad, W., Ihsanullah, 2019. Adsorption kinetics and modeling of H2S by treated waste oil fly ash. J. Air Waste Manage. Assoc. 69. https://doi.org/10.1080/10962247.2018.1536004.

Assi, A., Federici, S., Bilo, F., Zacco, A., Depero, L.E., Bontempi, E., 2019. Increased sustainability of carbon dioxide mineral sequestration by a technology involving fly ash stabilization. Materials 12. https://doi.org/10.3390/ma12172714.

Benassi, L., Zanoletti, A., Depero, L.E., Bontempi, E., 2019. Sewage sludge ash recovery as valuable raw material for chemical stabilization of leachable heavy metals. J. Environ. Manag. 245. https://doi.org/10.1016/j.jenvman.2019.05.104.

Biswas, B.K., Inoue, K., Harada, H., Ohto, K., Kawakita, H., 2009. Leaching of phosphorus from incinerated sewage sludge ash by means of acid extraction followed by adsorption on orange waste gel. J. Environ. Sci. 21, 1753–1760. https://doi.org/10.1016/S1001-0742(08)62484-5.

Boniardi, G., Turolla, A., Fiameni, L., Gelmi, E., Bontempi, E., Canziani, R., 2022. Phosphorus recovery from a pilot-scale grate furnace: influencing factors beyond wet chemical leaching conditions. Water Sci. Technol. 85, 2525. https://doi.org/10.2166/wst.2022.132.

Boniardi, G., Turolla, A., Fiameni, L., Gelmi, E., Malpei, F., Bontempi, E., Canziani, R., 2021. Assessment of a simple and replicable procedure for selective phosphorus recovery from sewage sludge ashes by wet chemical extraction and precipitation. https://doi.org/10.1016/j.chemosphere.2021.131476.

Boniardi, G., Volonterio, A., Canziani, R., Punta, C., Riva, L., Turolla, A., 2024. Cellulose-based nanostructured aerogels for leachate decontamination: towards sustainable phosphorus recovery from sewage sludge ash. J. Clean. Prod. 475, 143638. https://doi.org/10.1016/J.JCLEPRO.2024.143638.

Bonilla-Petriciolet, A., Mendoza-Castillo, D.I., Reynel-Ávila, H.E. (Eds.), 2017. Adsorption Processes for Water Treatment and Purification. Springer International Publishing, Cham. https://doi.org/10.1007/978-3-319-58136-1.

Bontempi, E., 2023. How to perform a material recovery sustainability evaluation preliminary to LCA? resources. ENVIRONMENT AND SUSTAINABILITY 9, 100074. https://doi.org/10.1016/J.RESENV.2022.100074.

Bontempi, E., 2017. A new approach for evaluating the sustainability of raw materials substitution based on embodied energy and the CO2 footprint. J. Clean. Prod. 162, 162–169. https://doi.org/10.1016/J.JCLEPRO.2017.06.028.

Chen, J., Zhang, J., Wang, W., Ma, X., Guo, Y., Sun, F., Wang, Y., 2020. Comparison of adsorption characteristics of acid-base modified fly ash to norfloxacin. Spectrosc. Lett. 53. https://doi.org/10.1080/00387010.2020.1766507.

Chen, Z., Ji, W., Huang, Y., Wei, Y., Lu, J., Liu, L., Poon, C.S., 2024. Upcycling municipal solid wastes to self-foaming glass-ceramics by chemical additive-free and rapid low-temperature sintering. J. Clean. Prod. 444, 141261. https://doi.org/10.1016/j.jclepro.2024.141261.

De La Torre, A.G., Bruque, S., Aranda, M.A.G., 2001. Rietveld quantitative amorphous content analysis. J. Appl. Crystallogr. 34. https://doi.org/10.1107/S0021889801002485.

Donatello, S., Tong, D., Cheeseman, C.R., 2010. Production of technical grade phosphoric acid from incinerator sewage sludge ash (ISSA). Waste Manag. 30. https://doi.org/10.1016/j.wasman.2010.04.009.

Ducoli, S., Fahimi, A., Mousa, E., Ye, G., Federici, S., Frontera, P., Bontempi, E., 2022. ESCAPE approach for the sustainability evaluation of spent lithium-ion batteries recovery: dataset of 33 available technologies. Data Brief 42. https://doi.org/10.1016/j.dib.2022.108018.

Ducoli, S., Zacco, A., Valentim, B., Zanoletti, A., Ye, G., Mousa, E., Bontempi, E., 2023. ESCAPE simplified approach designed to evaluate materials sustainability: the case of new adsorbent materials for activated carbon substitution. Sustain. Mater. Technol. 38, e00709. https://doi.org/10.1016/J.SUSMAT.2023.E00709.

Fiameni, L., Assi, A., Fahimi, A., Valentim, B., Moreira, K., Predeanu, G., Slăvescu, V., Vasile, B., Nicoară, A.I., Borgese, L., Boniardi, G., Turolla, A., Canziani, R., Bontempi, E., 2021. Simultaneous amorphous silica and phosphorus recovery from rice husk poultry litter ash. RSC Adv. 11. https://doi.org/10.1039/d0ra10120f.

Foo, K.Y., Hameed, B.H., 2010. Insights into the modeling of adsorption isotherm systems. Chem. Eng. J. https://doi.org/10.1016/j.cej.2009.09.013.

Gao, S., Wang, Q., Nie, J., Poon, C.S., Yin, H., Li, J., 2021. Arsenate(V) removal from aqueous system by using modified incinerated sewage sludge ash (ISSA) as a novel adsorbent. Chemosphere 270. https://doi.org/10.1016/j.chemosphere.2020.129423.

Gitari, W.M., Petrik, L.F., Etchebers, O., Key, D.L., Okujeni, C., 2008. Utilization of fly ash for treatment of coal mines wastewater: solubility controls on major inorganic contaminants. Fuel 87. https://doi.org/10.1016/j.fuel.2008.03.018.

Hassan, M.J., Islam, MdF., Akter, N., Uddin, MdN., Abir, A.Y., Aoun, S. Ben, Hasnat, M. A., 2021. Applicability of gypsum in selective removal of anionic dye molecules from aqueous medium. Appl. Water Sci. 11, 7. https://doi.org/10.1007/s13201-020-01336-7.

Herzel, H., Krüger, O., Hermann, L., Adam, C., 2016. Sewage sludge ash - a promising secondary phosphorus source for fertilizer production. Sci. Total Environ. 542, 1136–1143. https://doi.org/10.1016/j.scitotenv.2015.08.059.

Hessou, E.P., Jabraoui, H., Hounguè, M.T.A.K., Mensah, J.B., Pastore, M., Badawi, M., 2019. A first principle evaluation of the adsorption mechanism and stability of volatile organic compounds into NaY zeolite. Z. Kristallogr. Cryst. Mater. 234. https://doi.org/10.1515/zkri-2019-0003.

Ismail, G.A., Sakai, H., 2022. Review on effect of different type of dyes on advanced oxidation processes (AOPs) for textile color removal. Chemosphere. https://doi.org/10.1016/j.chemosphere.2021.132906.

Lee, S.B., Shin, H.S., Ryu, D.D.Y., Mandels, M., 1982. Adsorption of cellulase on cellulose: effect of physicochemical properties of cellulose on adsorption and rate of hydrolysis. Biotechnol. Bioeng. 24, 2137–2153. https://doi.org/10.1002/bit.260241003.

Li, L., Wang, S., Zhu, Z., 2006. Geopolymeric adsorbents from fly ash for dye removal from aqueous solution. J. Colloid Interface Sci. 300. https://doi.org/10.1016/j.jcis.2006.03.062.

Lopez-Ramon, M.V., Stoeckli, F., Moreno-Castilla, C., Carrasco-Marin, F., 1999. On the characterization of acidic and basic surface sites on carbons by various techniques. Carbon N. Y. 37, 1215–1221. https://doi.org/10.1016/S0008-6223(98)00317-0.

Losey, D.J., Sihvonen, S.K., Veghte, D.P., Chong, E., Freedman, M.A., 2018. Acidic processing of fly ash: chemical characterization, morphology, and immersion freezing. Environ. Sci. Process. Impacts 20. https://doi.org/10.1039/c8em00319j.

Lynn, C.J., Dhir, R.K., Ghataora, G.S., West, R.P., 2015. Sewage sludge ash characteristics and potential for use in concrete. Constr. Build. Mater. 98. https://doi.org/10.1016/j.conbuildmat.2015.08.122.

Mahieux, P.Y., Aubert, J.E., Cyr, M., Coutand, M., Husson, B., 2010. Quantitative mineralogical composition of complex mineral wastes - contribution of the rietveld method. Waste Manag. 30. https://doi.org/10.1016/j.wasman.2009.10.023.

Muryanto, S., Bayuseno, A.P., 2014. Influence of Cu2+ and Zn2+ as additives on crystallization kinetics and morphology of struvite. Powder Technol. 253. https://doi.org/10.1016/j.powtec.2013.12.027.

Nicastro, G., Fahimi, A., Dufresne, A., Vahidi, E., Punta, C., Bontempi, E., 2025. Eco-design of cellulose nanocrystals through ESCAPE method at lab-scale. Carbohydr. Polym. 369, 124310. https://doi.org/10.1016/J.CARBPOL.2025.124310.

Pan, S.C., Tseng, D.H., 2001. Sewage sludge ash characteristics and its potential applications. In: Water Science and Technology. https://doi.org/10.2166/wst.2001.0636.

Raii, M., Minh, D.P., Sanz, F.J.E., Nzihou, A., 2014. Lead and cadmium removal from aqueous solution using an industrial gypsum By-product. Procedia Eng. 83, 415–422. https://doi.org/10.1016/J.PROENG.2014.09.050.

Riva, L., Pastori, N., Panozzo, A., Antonelli, M., Punta, C., 2020. Nanostructured cellulose-based sorbent materials for water decontamination from organic dyes. Nanomaterials 10. https://doi.org/10.3390/nano10081570.

Samsami, S., Mohamadi, M., Sarrafzadeh, M.H., Rene, E.R., Firoozbahr, M., 2020. Recent advances in the treatment of dye-containing wastewater from textile industries: overview and perspectives. Process Saf. Environ. Prot. https://doi.org/10.1016/j.psep.2020.05.034.

Shindhal, T., Rakholiya, P., Varjani, S., Pandey, A., Ngo, H.H., Guo, W., Ng, H.Y., Taherzadeh, M.J., 2021. A critical review on advances in the practices and perspectives for the treatment of dye industry wastewater. Bioengineered. https://doi.org/10.1080/21655979.2020.1863034.

Singh, A., Sonal, S., Kumar, R., Mishra, B.K., 2020. Adsorption of chlorhexidine digluconate on acid modified fly ash: kinetics, isotherms and influencing factors. Environ. Eng. Res. 25. https://doi.org/10.4491/eer.2018.412.

Sulistiyo, Y.A., Andriana, N., Piluharto, B., Zulfikar, Z., 2017. Silica gels from coal fly ash as methylene blue adsorbent: isotherm and kinetic studies. Bull. Chem. React. Eng. Catal. 12. https://doi.org/10.9767/bcrec.12.2.766.263-272.

Trong, V.M., Tuan, V.M., Chinh, N.T., Giang, N.V., Trang, N.T.T., Thanh, D.T.M., Hang, T.T.X., Hoang, T., 2015. Characterization of fly ash modified with vinyltriethoxysilane. J. Nanosci. Nanotechnol. 15. https://doi.org/10.1166/jnn.2015.9525.

Wang, Q., Li, J. shan, Poon, C.S., 2019. Using incinerated sewage sludge ash as a high-performance adsorbent for lead removal from aqueous solutions: performances and mechanisms. Chemosphere 226. https://doi.org/10.1016/j.chemosphere.2019.03.193.

Wang, S., Soudi, M., Li, L., Zhu, Z.H., 2006. Coal ash conversion into effective adsorbents for removal of heavy metals and dyes from wastewater. J. Hazard. Mater. 133. https://doi.org/10.1016/j.jhazmat.2005.10.034.

Ye, Y., Ngo, H.H., Guo, W., Liu, Yiwen, Li, J., Liu, Yi, Zhang, X., Jia, H., 2017. Insight into chemical phosphate recovery from municipal wastewater. Sci. Total Environ. 576, 159–171. https://doi.org/10.1016/J.SCITOTENV.2016.10.078.

Yin, G., Song, X., Tao, L., Sarkar, B., Sarmah, A.K., Zhang, W., Lin, Q., Xiao, R., Liu, Q., Wang, H., 2020. Novel Fe-Mn binary oxide-biochar as an adsorbent for removing Cd (II) from aqueous solutions. Chem. Eng. J. 389, 124465. https://doi.org/10.1016/J.CEJ.2020.124465.

Zanoletti, A., Cornelio, A., Bontempi, E., 2021. A post-pandemic sustainable scenario: what actions can be pursued to increase the raw materials availability? Public Health Emergency 202, 111681. https://doi.org/10.1016/j.envres.2021.111681.